IEEE Access
Multidisciplinary | Rapid Review | Open Access Journal

Received October 13, 2020, accepted October 29, 2020, date of publication November 4, 2020, date of current version November 16, 2020.

Digital Object Identifier 10.1109/ACCESS.2020.3035871

iCrawl: An Inchworm-Inspired Crawling Robot

MUHAMMAD BILAL KHAN[1], THIRAWAT CHUTHONG[1], CAO DANH DO[2], MATHIAS THOR[2], PETER BILLESCHOU[2], JØRGEN CHRISTIAN LARSEN[2], AND PORAMATE MANOONPONG[1,2], (Member, IEEE)

[1]Bio-Inspired Robotics and Neural Engineering Laboratory, School of Information Science and Technology, Vidyasirimedhi Institute of Science and Technology, Rayong 21210, Thailand

[2]Embodied AI and Neurorobotics Laboratory, SDU Biorobotics, The Mærsk Mc-Kinney Møller Institute, University of Southern Denmark, 5230 Odense, Denmark

Corresponding author: Poramate Manoonpong (poramate.m@vistec.ac.th)

This work was supported by a startup grant on Bio-Inspired Robotics from the Vidyasirimedhi Institute of Science and Technology (VISTEC) (Project PI: Poramate Manoonpong).

ABSTRACT Inchworms use their morphology and evolved behaviors to crawl and climb various complex surfaces. This has inspired the development of different robots that can demonstrate similar capabilities for various applications such as the inspection of a complex environment. One of the key challenges in designing these robots is to enable them to be practically deployable with a compact design for providing continuous adaptability to a complex terrain such as an outer-pipe surface. Taking this into consideration, we present a new design for an inchworm-inspired crawling robot (iCrawl). The 5 DOF robot relies on two legs; each with an electromagnetic foot, in order to crawl on the metal pipe surfaces. The robot uses a passive foot-cap underneath an electromagnetic foot, enabling it to be a versatile pipe-crawler. The foot-cap design is an abstraction of the leg posture in an inchworm adapting to a round surface. The proposed foot-caps give the robot adaptability and stability for crawling on metal pipes of various curvatures. A state-machine based controller was developed to produce the required motor signals for the two inchworm-inspired crawling gaits: i) the step gait, and ii) the sliding gait. Both gaits were tested on the robot, eventually leading to it effectively crawling on the pipes and flat surfaces, climbing a metal wall and a pipe, and succeeding in obstacle avoidance during crawling. Experimental results also show that the robot has the ability to crawl on the metal pipes of various curvatures using the foot-caps and an appropriate gait. The robot can be used as a new robotic solution to assist close inspection outside the pipelines, thus minimizing downtime in the oil and gas industry.

INDEX TERMS Pipe-crawling robot, bio-inspired legged robot, locomotion control, tele-autonomous system, robot gait design, magnetic adhesion, inspection robot.

I. INTRODUCTION

Legged creatures are amazing locomotion models found in nature. From insects to animals and humans, their morphology and evolved behaviors of crawling, climbing, swimming, and walking on various complex terrains allow them to perform adaptive and more complex forms of such locomotion. This has inspired the development of various bio-inspired robots that imitate certain physical as well as behavioral attributes of the legged creatures [1]. With the intention of solving real-world problems, various efforts focus on learning the biology as well as behavior of legged creatures. An inchworm is one such interesting creature, using its legs and flexible body to perform adaptive crawling on different complex terrains. Several previous works report the biological aspects of different caterpillars including an inchworm [2]–[6]. Building on the existing understanding of an inchworm's biology, various robots have been developed [7]–[15]. Such robots mimic the construct as well as the locomotion pattern of an inchworm.

There are multiple benefits to using an inchworm as an inspirational model for a robot. Foremost, an inchworm-inspired robot can perform robust locomotion using two legs [8], [9], [16]–[18]. Relying on minimum, yet sufficient, contact-to-surface by the legs, a robot may require minimal hardware for its development in comparison to other

The associate editor coordinating the review of this manuscript and approving it for publication was Yingxiang Liu.

This work is licensed under a Creative Commons Attribution 4.0 License. For more information, see https://creativecommons.org/licenses/by/4.0/

robots [1] with more than two legs. With an effective adhesive surface mechanism and motor configuration, a robot can negotiate most terrains and obstacles. It is challenging to control such a robot due to the bi-legged motor configuration. However, a robot can leverage its bi-legged compactness and motor- configuration versatility for effective locomotion to solve real-world problems in a complex real-world environment.

A major challenge in the oil and gas industry is the constant maintenance and thereby effective inspection of pipelines [19], [20]. These pipelines are an example of a complex environment, involving a high safety risk to human site-inspectors. It is challenging to obtain the necessary information on oil or gas leakages, pipe corrosion levels, or other pipeline failures without an effective remote monitoring method to assist the site-inspector. This is due to the large area over which a pipeline might be spread, as well as the complexity involved in inspecting narrowly placed pipelines under harsh weather conditions, thereby limiting or denying human access. A few solutions may help to resolve the problem to some extent [20]. For example, using a still camera for general on-site activity monitoring or employing a drone for aerial inspection. However, both options have limitations. Monitoring with a still camera can give a fair amount of information on the scene but fails to accurately provide more critical information such as pipeline leakage. Also, depending on the spread of a pipeline, a network of cameras may require considerable infrastructure support and hence increased installation and maintenance costs. On the other hand, drones can provide aerial inspection of a pipeline, although existing long-distance sensing methods in a cluttered environment may restrict their practical reach [21].

To solve this need to have near-to-scene or close pipe inspection, we propose a new design for an inchworm-inspired pipe-crawling robot (Fig. 1). We focus on how the robot can be deployable in the real-world through the proposed development. The robot has five motor joints and two electromagnetic feet. We developed passive foot-caps for the robot in order for it to effectively and stably crawl on metal pipes of various diameters. The robot uses two gaits, the first of which is based on a step-like robot movement. The second gait is based on the sliding movement of the robot. The robot utilizes a state-machine-based controller for each gait. First, it is tested on *painted* metal pipes and a flat metal plate. The robot was then tested on *non-painted* metal surfaces to examine any underlying correlation between the effectiveness of the employed gaits and surface-type.

Outer-pipe inspection using a robot crawler is challenging [20]. This is due to the complex curved shape of a pipe. Hence, it involves more complexity than other existing and comparatively less challenging solutions for deploying a robot inside a pipe. In an onshore oil and gas pipeline, we can only consider deploying a robot outside the pipe's surface in order to monitor external leakages or other useful information and downtime [20], [22]. Considering this, the paper makes the following contributions:

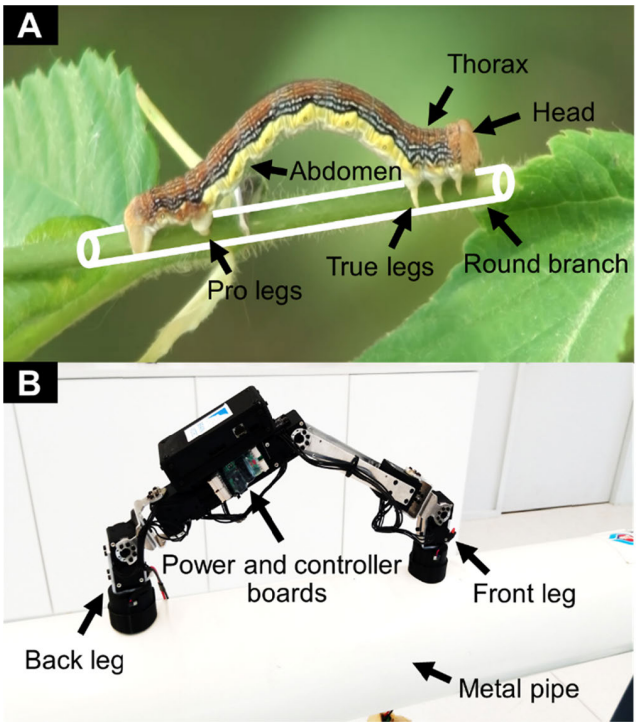

FIGURE 1. iCrawl robot is inspired by the structure and locomotion behavior of an inchworm. A) Linden Looper Moth (Geometridae: Erannis tiliaria) inchworm with its crawling posture on a plant branch (photo courtesy of Carl Barrentine). B) iCrawl robot with its crawling posture on a metal pipe.

- Development of minimal hardware, relying on the versatile design of an inchworm-inspired crawling robot. The robot is designed to match the compactness required for real-world deployment.
- Passive foot-cap design, enabling the robot feet to adhere to metal pipes of various curvatures. This gives the robot considerable leverage, making it a versatile pipe-crawler for multi-diameter pipes, thereby, avoiding the need to replace or adjust the foot design for each pipe.
- Development of two gaits that mimic step and sliding-like movements; each with its stated advantages and use-scope for outer-pipe robot locomotion.
- Successful demonstration of the robot crawling on metal pipes of different curvatures, employing the suggested tested conditions.
- Practically achievable recommendations, enabling the robot to crawl out of a lab environment into a real-world pipeline inspection scenario.

II. RELATED WORK

Several studies consider the design of inchworm-inspired crawling robots using different approaches and scope of applications. For instance, a foldable inchworm-inspired robot demonstrated the ability to crawl on a non-metal plain surface at a speed of 2 mm/s. The robot exploited the Joule heating effect using the shape memory polymers on the embedded circuits [23], without employing a surface

adhesion method. Another robot, called Omegabot, performed worm-like flat surface crawling at a speed of 9 mm/s by bending its body into an omega shape, using SMA spring actuators and anisotropic friction pads [11]. Two modular caterpillar-inspired wall climbing robots were developed by [12] to perform crawling on a flat surface using passive suckers for surface attachment. While another caterpillar-inspired wall climbing robot demonstrated climbing with the use of its four body segments; each with a solenoid actuator and permanent magnet plunger [13]. The robot used polydimethylsiloxane (PDMS) gecko-inspired pads for attachment of the head and body segments. It was able to climb up to a speed of 10.07 mm/s. A flat surface climbing robot was developed to assist inspection of steel bridges [24]. The robot climbed the flat steel surface using foot-pads; each attached with three magnetic toes. A wall climbing robot was developed on the basis of vacuum adsorption feet [25]. The sucker modules were aligned such that an airtight chamber was obtained to generate the vacuum. Recently, a caterpillar-inspired soft robot was developed to crawl on tree branches of up to 1.27 cm in diameter [14]. The robot used three tendon-based passive grippers; each actively released by an independent motor. The deformable soft body of the robot supported it to conform well on a branch.

Other legged and wheeled robots have shown various levels of crawling and climbing over surfaces, mainly relying on biomimetic adhesives, magnetic adhesion, or mechanical grippers for attaching to a surface. For example, one four-legged glass-surface climbing robot used dry adhesive pads for attachment [26]. Another robot was introduced with magnetic wheels to attach to thin and flat metal surfaces [27]. A four-legged robot, called Magneto, climbed a flat metal surface using electromagnetic feet [28], while a radio-controlled robot used magnetic adsorption to attach and crawl inside the metal pipes [26]. Another robot used eight flat dry adhesive-based foot-pads connected to a motor actuated by four-bar mechanism [29]. The robot climbed flat and certain changing-curvature walls, up to a speed of 1.25 cm/s. A four-legged robot used a passive spine gripper at the end of each robot-leg to climb cliff walls [30]. These examples broadly represent recent advancements in crawling and climbing robots.

To summarize, existing worm-like or other similar robots have mainly targeted flat surfaces (horizontal crawling or vertical climbing) [11], [13], [15], [23]–[25], [27], [28], [31], [32] (see also discussion section) or in-pipe locomotion [33]–[35]. Outer-curved surface crawlers relied on gripping mechanisms to demonstrate crawling behavior while also indicating their grippers' fixed grasping range [11], [25], [26]. Moreover, some of these robots were either large and bulky[20], [36], or developed as prototypes to demonstrate the design concepts and hence required further development for real-world deployment [7], [9], [11], [14], [16], [17], [23], [25], [27], [29], [30], [35]. Recent works based on advancements in soft robotics may help to achieve a more effective design solution [14]. However, despite the promising initial developments, most works show practical limitations at this stage for real-world scenarios such as the one targeted here—a multi-diameter metal-pipe crawling robot for the inspection of oil and gas pipelines (Fig. 2).

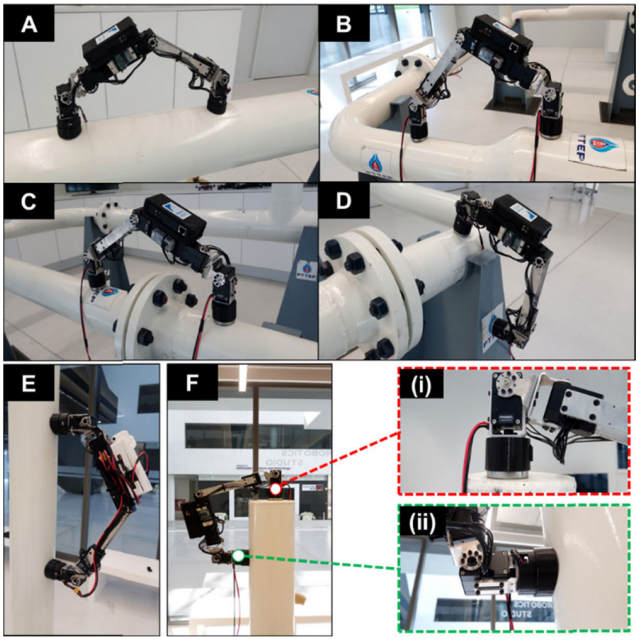

FIGURE 2. Various iCrawl postures on the metal pipes, demonstrating some of the situations it may come across during the inspection of a pipeline. The robot design enabled it to crawl on metal pipes of different diameters and flat surfaces. A) iCrawl in a crawling posture on a pipe. B) iCrawl in a transitioning posture between two pipes of different diameters. C) iCrawl posture when crossing an obstacle. D) iCrawl in a transitioning posture from a flat surface onto a pipe. E, F) The robot in a climbing posture, and in a close-end scenario involving flat and curved surfaces. (i) and (ii) show the robot feet without and with the cap, respectively.

III. MATERIALS AND METHODS

A. THE ROBOT DESIGN

The robot design is primarily based on the following two ideas:

i. Enabling the robot to rely on minimum degrees of freedom (DOF) to achieve versatile movements
ii. Adding a passive yet effective foot-to-surface adhesive mechanism, resulting in stable robot behavior, while crawling on metal pipes of various curvatures.

We considered achieving robot versatility using five DOFs in the bi-legged robot body configuration (details in the next sub-section). Although the presented motor configuration made the control challenging, it delivered compactness leverage as part of robot deployment criteria. Overall, the design provided further leverage when combined with the gait control design; each complementing the other.

In order to obtain foot-to-surface adherence, we developed a passive foot-cap underneath the electromagnetic foot. The foot-cap was inspired from the construct of an inchworm's legs. Our design generalization did not fully imitate an inchworm's leg which has complex underlying biology, rather we

TABLE 1. Specifications of the robot.

Specification	Details
Dimensions	Length = 56 cm, Width = 4 cm
Weight	1.42 kg (with battery onboard)
Total DOF	5
Actuation type	Electrical (Dynamixel XM430-W350-R)
Communication and controller boards	1. U2D2 (communication with computer) 2. Arduino nano (magnet drive controller)
Sensors	1. Dynamixel Internal encoders 2. Hall sensors at the feet 3. A current sensor (ACS712, 20A)
Power	A 3 cell LiPo battery (12V, 3000mAh)
Foot adhesion method	2 Electromagnets (5.3W, 470N, 12V)

considered an abstractive way to use some of the relevant attributes to achieve the surface adherence objective through the proposed passive foot-cap. The extended details of the robot design are presented below.

1) INCHWORM BODY-INSPIRED ROBOT BODY

We used a combination of 3D printing and CNC machining to build the robot skeleton. The 3D printed robot links were made of ABS and PLA thermoplastics, whereas aluminum assemblies were prepared using a laser cutter and a CNC machine. The robot was equipped with five servo motors; each configured to achieve a safe yet sufficient operating angle for the desired robot crawling. The overall iCrawl skeleton design was an abstractive imitation of an inchworm. Relying on the five servos in the bi-legged configuration, the robot obtained extra reach in the joint workspace. This allowed it to be versatile in various practical situations. Figure 3 shows various aspects of the robot design.

The robot uses an electromagnet underneath each foot in order to provide sufficient adhesion to a metal surface. We chose this for two reasons:

1. The robot has to crawl on metal surfaces. An obvious but effective choice is to use electromagnetic adhesion. The flux switching electromagnets are permanent, hence they *only* require power to detach from a metal surface; reducing overall robot power consumption. This also ensures that the robot does not fall over during a power outage event by relying on magnetic adhesion.
2. In comparison to other methods for the adhesion of robot feet on *metal surfaces* as discussed in section 1, magnetic adhesion outperforms other methods in terms of deployment. This is under the assumption that we consider the system to be driven all-electrically with onboard equipment. This also allows the iCrawl robot to meet the design criteria of compactness, as well as making it an electrically driven system.

Table 1 lists the key hardware elements of the iCrawl robot. Since design of the robot's feet is fundamental to its crawling ability, the details are described below.

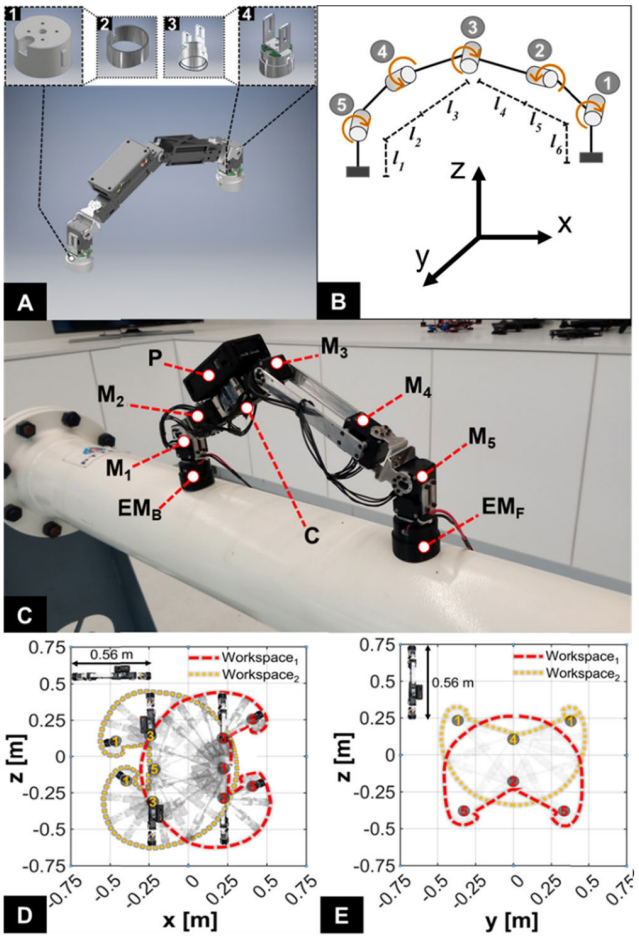

FIGURE 3. Compact design of the robot, relying on different features. A) The CAD design of the robot indicating: (1) a magnet housing, (2) a foot-cap, (3) a foot-cap wrapped around the magnet housing, (4) a complete robot foot. B) Indication of robot motor-rotation and body segment lengths. $M_{1,3,5}$ rotate around the x axis while $M_{2,4}$ rotate around the z axis. The robot link lengths shown are: $l_{1,6} = 10$ cm, $l_{2,5} = 6$ cm, $l_3 = 15$ cm, and $l_4 = 9$ cm. C) iCrawl's $M_{1,3,5}$ motor joints are kept in an active state for a unidirectional worm-like movement, while, $M_{2,4}$ motor joints are fixed at a certain angle. C is the U2D2 that provides an interface for a PC to communicate with the servos. P is the power source connector. The $EM_{F,B}$ are permanent electromagnetic feet mounted under the front and back legs to provide switchable adhesion to the metal surface. D) and E) show the robot workspace/overall reachability when either of its ends (M_1 or M_5) are considered.

2) INCHWORM LEG-INSPIRED ROBOT FEET

We considered the robot foot design by looking at an inchworm's ability to grasp and crawl different surfaces using its legs. An inchworm uses multiple pairs of legs to adapt to a surface. During crawling, its legs act as a side-hook to a surface (each pair of opposite-side legs provides the grasp to a surface). During this stage, the body segment in the middle of any pair of opposite-side legs may appear as curve-shaped, given that the inchworm is crawling on a curved surface. The robot feet were developed by considering this as the design motivation (Fig. 4).

The robot feet were designed particularly for curved metal surfaces, and hence met the following requirements:

1. To provide the robot with the necessary surface adhesion using electromagnets.

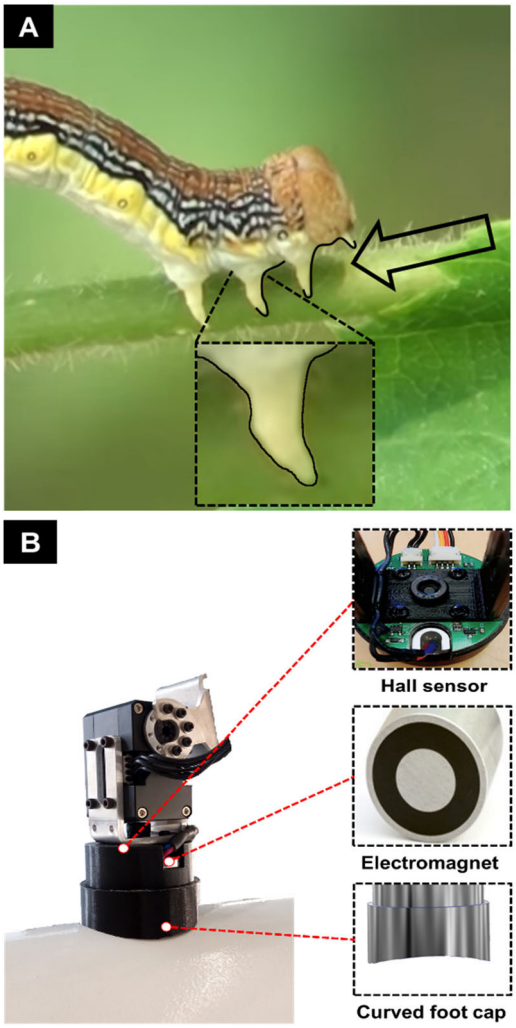

FIGURE 4. Inchworm leg-inspired robot foot structure. A) Close-up of an inchworm's leg appearing as a side-hook, and a front view indication of its opposite pair of legs appearing to be curve-shaped. This helps it to stably grasp a round surface. B) The robot foot with an electromagnet covered by the curved foot-cap at the bottom. The foot-cap is based on an abstractive imitation of an inchworm's legs when crawling on a round branch. A hall sensor is installed on the top of the foot. The curved cap allows the robot to stably walk on curved surfaces (i.e., a pipe with a diameter of between 12 and 22 cm).

2. To help the robot distinguish between a metal and a non-metal surface using hall sensors.
3. To make the robot feet passively adapt to a curved pipe by using the curved foot-caps underneath the electromagnets.

A hall sensor was mounted on top of the electromagnet to distinguish the robot crawling surface. It acts on the hall sensor effect with varying output voltages based on the intensity of the magnetic flux around it. This flux was detectable by the hall sensors. Table 2 lists the sensor outputs that help to distinguish the metal and non-metal robot crawling-surfaces.

A 3D printed curved cap was designed to wrap the electromagnet. The foot-cap was used so as to provide side-to-side surface adaptability for the robot foot, resulting in two advantages: 1) Reducing slippage of the magnetic foot during foot detachment, thereby increasing robot stability during crawling; and 2) Obtaining sufficient adhesive force to move on different curved pipe surfaces. The foot-cap proved to be an effective add-on to make the robot crawl on different metal pipes with diameters of between 12 and 22 cm.

TABLE 2. The hall sensor output on metal and non-metal surfaces.

Power state	Magnet state	Sensor output	Surface interpretation
OFF	ON	0.78 V	*Metal*
OFF	ON	0.94 V	*Non-metal*
ON	OFF	0.99 V	*N/A (Demagnetized scenario in crawling)*

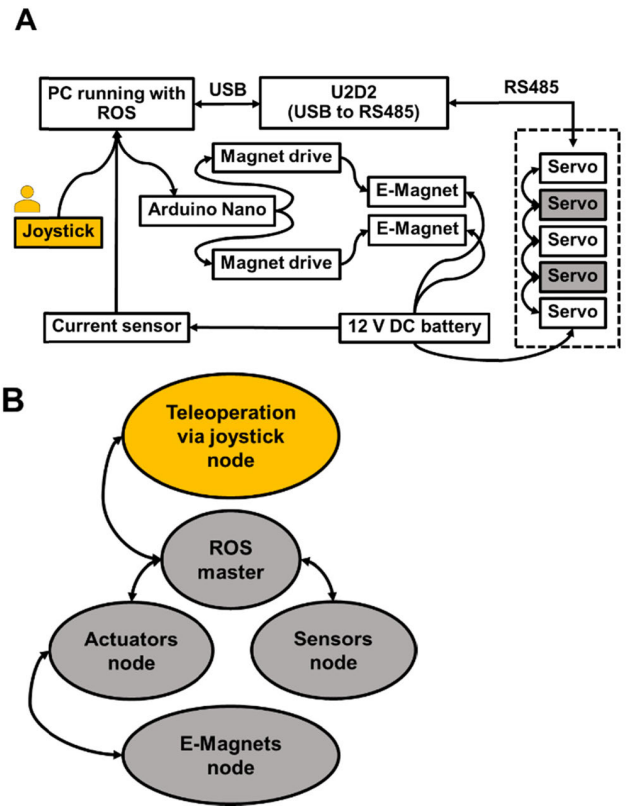

FIGURE 5. A) The system hardware diagram showing the hardware interfacing. B) The ROS node diagram indicating the software-end development. A joystick node was activated only in the tele autonomous mode.

3) ROBOT HARDWARE AND SOFTWARE INTERFACES

Figure 5 (A) presents an overview of the robot hardware and software interfaces. A personal computer (PC) was used as the remotely accessible top-level controller. Using a USB and RS485 Dynamixel controller, we serially connected all the servo motors of the robot. A 12 V LiPo battery powered the electromagnets and servos. The electromagnets were switched using a relay (magnet drive) through an Arduino Nano connected to the PC running with the robot operating system (ROS). A joystick was also used in the teleoperated robot locomotion experiments.

We used the ROS to program the robot. Figure 5 (B) illustrates various nodes in the ROS program. The ROS master provides naming and registration services to the sensor, actuators, and teleoperation nodes. The actuator node subscribed and published simultaneously to the electromagnets' node. The joystick inputs (in the teleoperated robot control experiment), motor position, sensor states, and electromagnet states were the baseline parameters to develop the gait controllers as described in the following section.

B. ROBOT LOCOMOTION CONTROL

The robot locomotion control is based on position control. The crawling behavior of the iCrawl robot is based on an inchworm-like crawling. An inchworm uses its legs to anchor to a surface. Using a cyclic movement, it crawls on different surfaces. First, the front legs (true legs) attach to the surface while the back legs (prolegs) become detached. It then uses its abdominal muscles to produce a loop-like shape. Now, the front legs detach while the back legs attach to the surface. Finally, the abdominal muscles are used to straighten up the body for a complete step [11], [18]. Using an inchworm's movement behavior as the motivation for robot locomotion control, we developed two gaits to enable robot crawling: 1) the stepping gait; and 2) the sliding gait. Figure 6 shows the motor joint signals, magnet switching signals, and diagrams for both gaits.

These two gaits were developed to enable the robot to crawl on flat and curved surfaces. By adding the necessary modifications, these were extended for complex scenarios such as vertical robot climbing on flat and curved metal surfaces, as well as negotiating an obstacle avoidance scenario on a metal pipe. In the following section, the robot gaits and their application scenarios are described in detail.

1) STEPPING GAIT CONTROL

The stepping gait state-machine controller is illustrated in Figure 7 (A). To make the robot perform unidirectional crawling, motor joints $M_{1,3,5}$ were controlled using the state-machine controller. First, we detached one of the feet. Each state-transition to the next step was defined as a separate state (six states in total: S_1 to S_6, for a single step as shown in Figure 7 (A)). We recorded the joint angles of each state manually by statically placing the robot in the desired crawling state. By noting the joint angles of all motors, these could be played back later through the feedforward state-machine controller. The magnetic switching followed the gait pattern. However, the magnet ON duration during the swing phase was kept to a minimum in order to prevent overheating. This gait was designed to obtain a slow but stable robot foot landing; abstracting an inchworm-like movement. This gait can be extended to allow the robot to use a sensor-mounted front leg for active sensing [37].

Apart from crawling on horizontal surfaces using the stepping gait, we modified the gait-controller for vertical robot climbing as well. This was done by reducing the step height and increasing the duration of a complete step. By doing so,

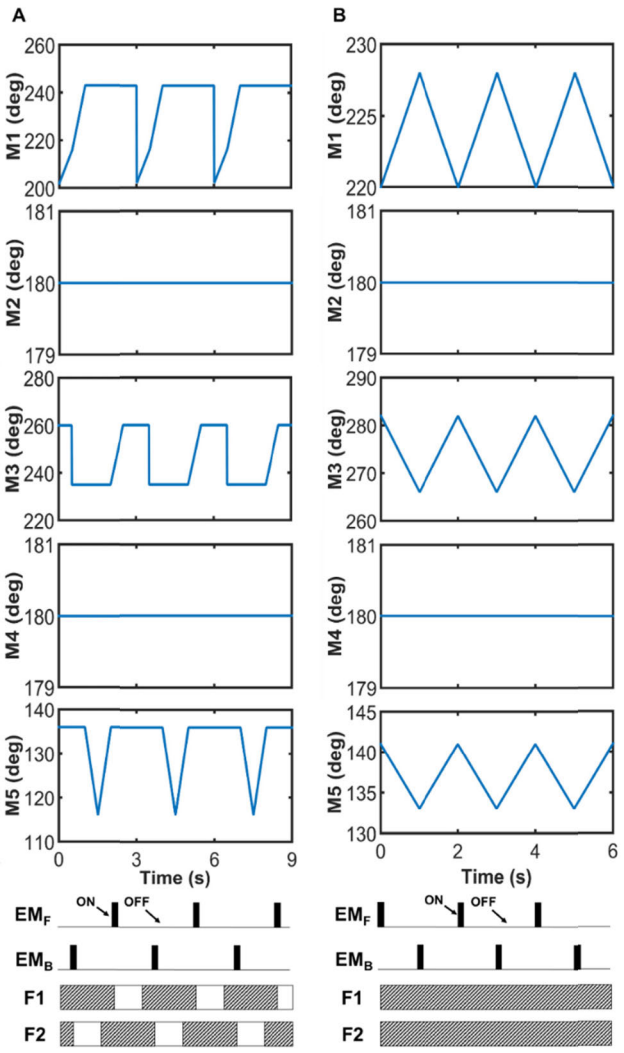

FIGURE 6. Using the stepping gait (gait 1) and the sliding gait (gait 2), the robot performed unidirectional crawling. A) Motor signals that produce gait 1 (a step-like robot movement), magnet switching pattern, and the gait diagram of both feet (here referred to as F1 and F2). B) Motor signals that produce gait 2 (a sliding-like robot movement), magnet switching pattern, and the gait diagram of both feet.

the robot's center of mass remained nearer to the climbing surface. This was to counterbalance the robot weight when relying on one foot being attached and the other detached; allowing the robot feet to hold onto the surface. An increase in the step duration for vertical climbing reduced robot body oscillations during magnetic switching while improving robot stability. Both gait variations were developed to enable the robot to step over an obstacle when crawling on a pipe.

2) SLIDING GAIT CONTROL

The sliding gait was inspired by an inchworm's two-anchor crawl [11], [18], achieved by developing the gait in only two states. Figure 7 (B) shows the state-machine loop of the two states for the sliding gait. Here, all three motor joints ($M_{1,3,5}$) are simultaneously controlled for unidirectional robot crawling. First, the robot detaches one of its feet, moving the

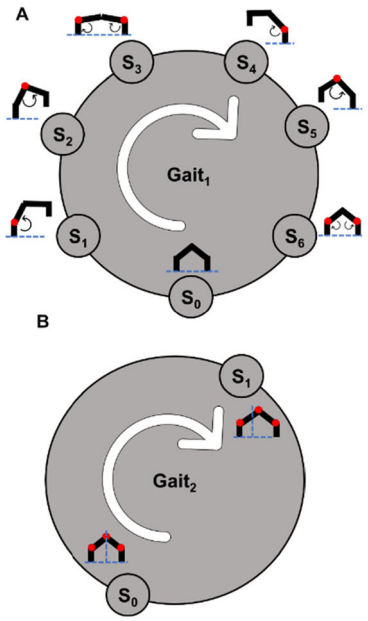

FIGURE 7. The iCrawl robot was tested using two crawling gaits. Each gait was different, based on the desired robot movement and hence composed of various states (each state represents a robot posture) as defined through the control scheme. A) An overview of the robot control using gait 1, yielding a step-like robot movement. B) An overview of the robot control using gait 2 to obtain a sliding-like robot movement.

motor joints simultaneously to perform a motion (state S_1 in Fig. 7 (B)). The back foot of the robot then follows the same pattern (state S_0 in the Fig. 7 (B)). During this movement, both robot feet stay inbound to the surface, making the robot perform sliding-based crawling.

3) POSTURE AND SEMI-AUTONOMOUS TELEOPERATION CONTROL

Both gaits (stepping and sliding) were designed as baseline movement patterns; enabling the robot to crawl and climb metal surfaces. The individual states in each gait were initiated using a feedforward control paradigm since this was a simple way to obtain the desired robot movement. However, it was challenging to obtain a continuous stable robot posture and successful point-to-point locomotion by solely relying on it. In robot crawling *on-pipe* scenarios, this was due to the robot body oscillations slowly deviating from a predefined crawling path, resulting in unsuccessful locomotion. To eliminate this, it was essential that the robot posture be corrected by steering it to align with the path. To achieve this, we activated the motor joints $M_{2,4}$ to enable steering of the robot legs. This steering behavior was then initiated using a joystick controlled by a human operator while teleoperating the robot in a testing scenario. At this stage, we did not use sensory feedback to obtain robot posture alignment.

The joystick controller was also effective in meeting the robot application in cases where a movement pattern is initiated remotely by a human. It acted as a teleoperation interface between a human operator and the robot. The human operator initiated robot crawling by having greater control over multiple locomotion parameters. These parameters included: robot speed, gait type, magnet states, specific movements such as stepping over an obstacle, and posture alignment to realign the robot following deviation from the desired path.

IV. EXPERIMENTS AND RESULTS

The robot was tested using three scenarios. Firstly, to crawl autonomously without any human intervention on horizontally placed painted industrial metal pipes of three different diameters (12, 16, and 22 cm) and a flat painted metal plate. Secondly, a non-painted metal pipe and a metal plate were used to observe differences in the robot's autonomous crawling. In both scenarios, the experiments were subdivided by testing the robot with and without foot-caps. These two scenarios were designed to analyze the effectiveness of the robot testing conditions such as foot design, appropriate gait, and surface compatibility. The third scenario further included complex environment situations such as vertical robot climbing on a metal wall and pipe. This scenario utilized the most appropriate robot testing conditions, following the first two scenarios in terms of testing surface and locomotion gait. The robot also negotiated an obstacle avoidance scenario using teleoperation in the semi-autonomous mode. The presented experiments were designed as test cases to investigate the effectiveness of the robot control; leveraging on its design.

We recorded and analyzed robot crawling behavior in all experiments. Through empirical evidence, the various insights gained are presented later in the discussion section of the paper. The experimental results are grouped in order to provide a compact comparative perspective on the robot performance as follows:

1. The robot crawling autonomously using the stepping gait (gait 1) and sliding gait (gait 2) on painted metal surfaces, with and without foot-caps (Fig. 8).
2. The robot crawling autonomously using the stepping gait (gait 1) and sliding gait (gait 2) on non-painted metal surfaces, with and without foot-caps (Fig. 9).
3. The robot climbing autonomously on a flat metal wall and non-painted metal pipe in a vertical direction (Fig. 10).
4. The robot stepping over an obstacle while crawling on a non-painted metal pipe, partially controlled by a human operator initiating crawling behavior (Fig. 11).

Figure 8 shows the robot being tested without foot-caps (denoted by N/C in the bar graphs) and with foot-caps (denoted by C in the bar graphs) to analyze the effectiveness of the proposed robot foot design. Both gaits were tested further to choose an appropriate gait to enable the robot to crawl effectively on the metal pipes. The robot crawled on the 12 cm (Fig. 8 (A)), 16 cm (Fig. 8 (B)), and 22 cm (Fig. 8 (C)) diameter pipes, as well as a flat metal surface (Fig. 8 (D)) with the corresponding crawling success (here referred to as the success rate: percentage of successful point-to-point robot locomotion in each scenario after five repetitions). The results show that gait 2 combined with the foot-caps

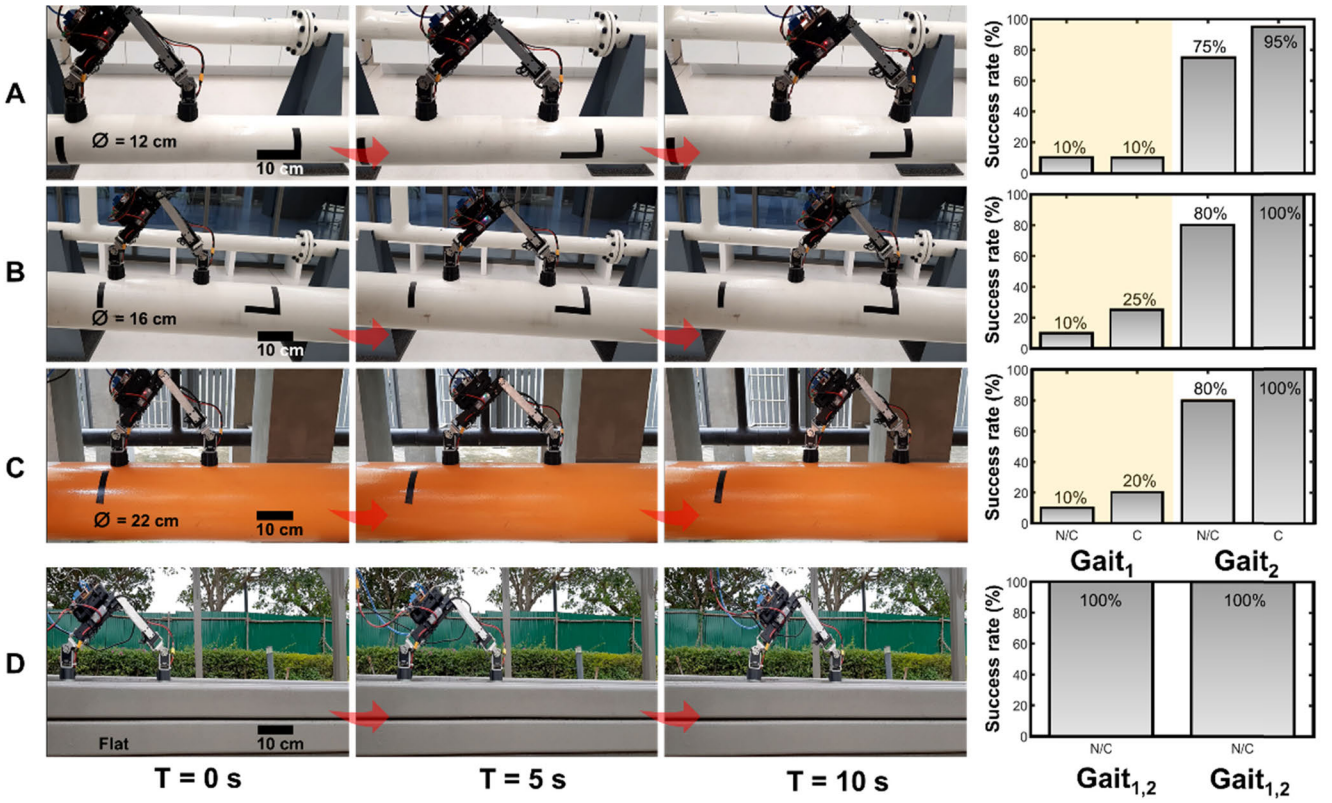

FIGURE 8. The robot was tested to crawl on different painted metal surfaces in various scenarios. A)–D) show the robot's crawling behavior in different conditions. The snapshots show the robot with an effective gait (i.e., gait 2 (sliding gait)). Note that in case D, the robot with foot-caps always failed to crawl on the flat surface (i.e., 0% success rate). The supplementary video of the experiment can be seen at www.manoonpong.com/icrawl/S1.mp4.

yielded effective robot crawling in all painted pipe surface scenarios.

The experiments reported in Figure 9 use the same settings as for the painted surface scenarios. The robot crawling with gait 1 improved on the non-painted metal pipe (Fig. 9 (A)) and the flat metal plate (Fig. 9 (B)).

The robot crawling results show the success rate for each scenario. The success rate is based on successful point-to-point crawling after five iterations in each testing scenario. Using the foot-caps and gait 2, the robot demonstrated better crawling behavior. The robot crawling proved to be less effective with gait 1 on the painted pipes in comparison to the non-painted. The results are further discussed in the next section.

V. DISCUSSION

The robot demonstrated different levels of crawling success in the tested scenarios. It performed better on the metal pipes when the foot-cap was used. However, its overall crawling success was also dependent on the type of crawling surface as well as the gait used. On the painted metal pipes measuring 12, 16, and 22 cm in diameter, the robot showed consistent improvement when the foot-cap was used (refer to the bar graphs in Fig. 8). Gait 2 also proved to be a key contributor to crawling success. This was because both robot feet were in stance and hence inbound to the surface at all times, in comparison to gait 1 which had a swing-stance. By using this stance-based gait, the robot was able to sustain its body weight. This contributed to stable and successful point-to-point crawling on the painted metal pipes. Interestingly, testing on the non-painted pipe revealed that gait 1 was also effective for robot crawling (Fig. 9). This was due to the absence of a paint layer on the metal pipe which gave enough adhesion to the electromagnetic feet thereby enabling the robot to sustain a stable weight during the swing. Essentially, gait 2 with the foot-cap is recommended for different diameter painted/non-painted pipes, while gait 1 can be used in part to obtain an extended-body posture during an active sensing-based path planning scenario [37]. It can allow the robot to transition from crawling horizontally to climbing vertically on an adjacent surface, building on the recent soft robotic demonstrations of similar behavior [29].

The robot crawled successfully on the flat painted and non-painted metal plates by employing both gaits. It was tested using the hypothesis that the robot may come across a flat surface and transition to a pipe or vice versa. Following the initial horizontal crawling scenarios, the robot climbed the vertical metal surfaces (Fig. 10). In this case, the robot performed well when we increased the step duration (slower movement). This results in stable climbing. In contrast to climbing on a flat metal wall, the robot was unstable at certain instances while crawling on the metal pipe. However, this

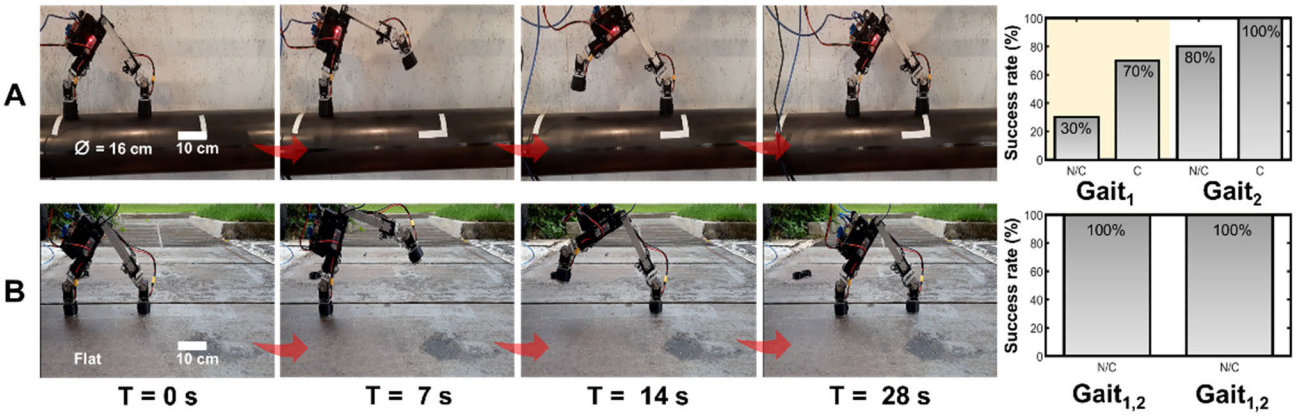

FIGURE 9. The robot was tested on non-painted metal surfaces to observe any differences in crawling behavior. A) and B) show the robot's crawling behavior in different conditions. The snapshots show the robot with gait 1 (stepping gait) to examine its stepping behavior. Note that in case B, the robot with foot-caps always failed to crawl on the flat surface (i.e., 0% success rate). The supplementary video of the experiment can be seen at www.manoonpong.com/icrawl/S2.mp4.

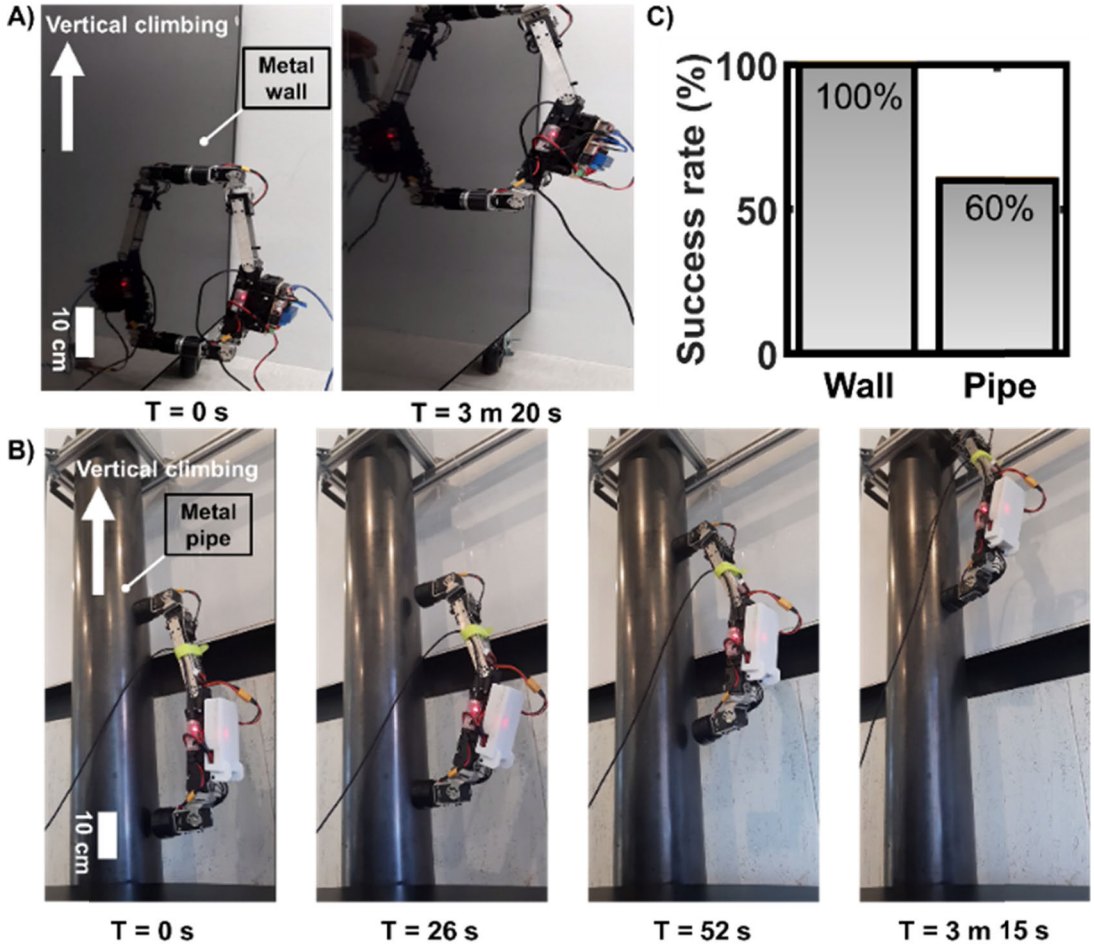

FIGURE 10. A vertical climbing scenario when the robot was tested on a flat metal wall and metal pipe. A) The robot climbing a metal wall. B) The robot climbing a metal pipe. C) The locomotion success rate of the robot climbing the wall and pipe between two points. The supplementary video of the experiment can be seen at www.manoonpong.com/icrawl/S3.mp4.

problem was solved by controlling the $M_{2,4}$ motor joints to keep the robot body aligned to the pipe centerline. A joystick was used to control the motor joints. This scenario provided the robot with the ability to climb tougher (toughness

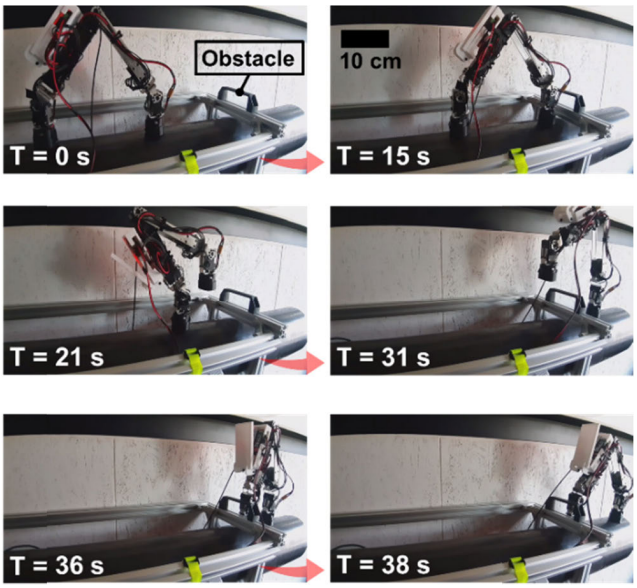

FIGURE 11. The robot stepping over an obstacle in its path on the metal pipe through teleoperation. A human operator only initiated the robot stepping over the obstacle behavior. The supplementary video of the experiment can be seen at www.manoonpong.com/icrawl/S4.mp4.

considering the robot crawling on the *pipe*) inclinations up to 90°. This was higher than a similar principle based on a two-anchor crawler that could climb a flat surface with a maximum inclination of 19° [18]. Finally, the obstacle avoidance scenario indicated the robot's versatility in negotiating an obstacle while performing semi-autonomous locomotion (Fig. 11). This could be the baseline behavior for extending the robot's functionality while crawling on a pipe with multiple flange-like obstacles.

Besides the robot's versatility in crawling horizontally, vertically, and crossing an obstacle, the robot also showed higher payload capacity by carrying up to 1.5 kg weight of batteries and a lifting mechanism mounted on top during the horizontal crawling. The robot also outperforms all existing worm-like robots by crawling on multiple large diameter (up to 22 cm) pipes without changing its physical properties. Additionally, the speed achieved is competitive to other robots reported in the existing literature. Figure 12 provides a comparative view of various worm-like robots and their properties as well as performance parameters.

To view the energy efficiency of the robot in the tested conditions, we calculated the cost of transport (COT), obtained through the following expression [11], [18]:

$$COT = \frac{IV}{mgv}, \tag{1}$$

where I is the average current in amperes consumed by the robot and measured by the current sensor while crawling for a distance of 1 m on all painted/non-painted surfaces, V is the battery voltage, mg is the weight of the robot, and v is the crawling speed of the robot in m/s. Figure 13 shows the cost of transport under various tested conditions.

It can be seen that the robot locomotion based on gait 2 costs less than that for gait 1. This was due to the various gait 1 states (S_1 to S_6) defined separately for a step, in comparison to the bi-state gait 2. The six states involved in a step using gait 1 took longer while increasing the load on each active motor as the robot lifted one of its legs. This effect was absent during gait 2 where the robot could robustly perform a step without lifting its body segment, hence reducing the load on the motors. Use of the foot-cap showed a slight difference

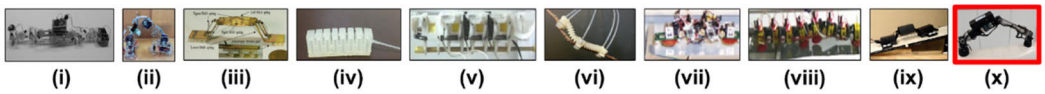

	(i)	(ii)	(iii)	(iv)	(v)	(vi)	(vii)	(viii)	(ix)	(x)
DOF	5	5	2	1	2	multiple	3	7	4	5
Weight (g)	Not reported	Not reported	1.2	Not reported	188	25.8	113.2	245.6	3930	1420
Actuation method	DC motors	Servo motors	SMA	Pneumatic	Solenoid	DC motors	Servo motors	Servo motors	Dynamixel motors	Dynamixel motors
Maximum payload (g)	None	None	None	50	None	None	25	80	450	Up to 1500
Attachment mechanism	None	Suction cups	Friction pads	None	Gecko pads	Soft grippers	Vacuum suckers	Vacuum suckers	Friction pads	Magnetic
Speed (mm/s)	Not reported	Not reported	10	2.2	Up to 12.4	0.75	2.4	1.75	25.4	25
Crawling surface	Flat	Flat	Flat	Flat	Flat	Round (up to 12.7 mm diameter)	Flat	Flat	Flat	Flat, and round (up to 220 mm diameter)
Crawling capability	Horizontal crawling & obstacle crossing	Horizontal crawling only	Horizontal crawling only	Horizontal crawling only	Horizontal & vertical crawling	Horizontal & vertical crawling	Horizontal & vertical crawling	Horizontal & vertical crawling	19° inclined surface crawling	Horizontal crawling with obstacle crossing & vertical (up to 90° inclined surface) crawling

FIGURE 12. A comparative view of state-of-the-art worm-like robots (i-ix) and our robot (x) based on various functional parameters. Our robot is highly versatile with superior payload capacity and competitive crawling speed while crawling on curved surfaces with up to 22 cm diameter. Other robots shown here are reported from the literature in this order: (i) reported in [7], (ii) in [8], (iii) in [11], (iv) in [12], (v) in [13], (vi) in [14], (vii) in [15], (viii) in [15], and (ix) in [18], whereas (x) is our robot which is presented in this article.

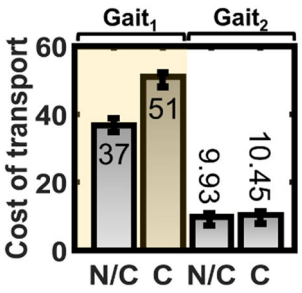

FIGURE 13. The cost of transport (COT) associated with the robot crawling using gaits 1 and 2.

in the COT due to the extra current consumed by the $M_{1,5}$ motor joints. This was based on the extended plastic slit of the passive foot-cap which acted against the magnet's attachment direction, resulting in a jolt and hence a minor increase in the motor current consumption.

Currently, the robot relies on electromagnetism for metal-surface adhesion. The magnets used in the robot feet come with their factory-provided ratings. However, to obtain an estimate of the effective adhesion for each tested metal surface, we conducted a small experiment using a weight scale. By attaching and then linearly pulling the robot foot from the tested surface using the weight scale, we noted the effective available robot foot adhesion (Fig. 14). Each adhesion experiment was repeated five times for all the tested surfaces.

In the adhesion experiments, we noted that the increase in adhesion was consistent with the increase in the testing pipe diameter in all painted metal-surface crawling scenarios. With an increase in pipe diameter, the magnet could obtain the maximum surface-contact area and hence higher adhesion. Use of the foot-cap did not have any direct influence on the adhesion. However, it provided a firmer surface attachment to the magnet, which proved to increase the magnet's grip to the surface. This resulted in slightly higher adhesion than without use of the foot-cap. On the non-painted tested surfaces, this was similarly noted. However, it was found that the magnetic adhesion was approximately five times higher when tested on the non-painted metal surfaces, in comparison to the painted surfaces. This showed that the paint coatings on the tested surfaces largely influenced foot adhesion; ultimately proving to be one of the leading factors impacting on the success of robot crawling. This supports Figure 9 where the robot shows a higher crawling success rate on the non-painted metal surfaces when driven through gait 1 (or the stepping gait). The available higher magnetic adhesion on such surfaces contributes to the robot being able to sustain its weight while attaching only one of its legs onto a metal surface. These observations further assist in electromagnet selection with respect to required adhesion, testing surface type, robot weight, and total available adhesion of the employed electromagnets.

The robot speed was not considered at this stage as a key performance criterion due to our focus being on the robot's capability to stably crawl and climb the curved surfaces. However, as the speed depends on the step length and

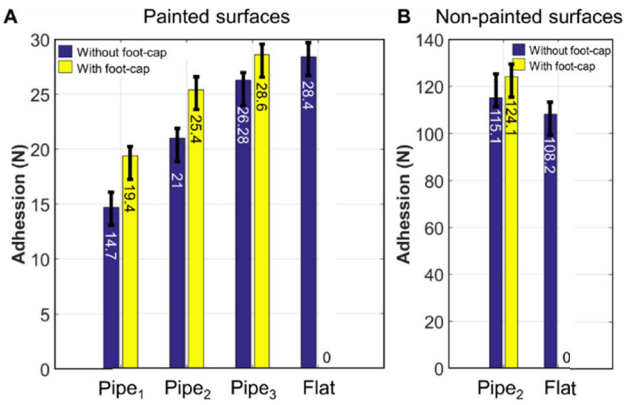

FIGURE 14. The electromagnetic adhesion available on each robot foot through the respective electromagnets. Here, metal pipes1,2,3 measure 12, 16, and 22 cm in diameter, respectively. On the flat metal plates, with the foot-cap, the effective adhesion is zero as it restricts exposure of the magnet to the flat metal surface.

joint frequency, it can be adjusted accordingly as part of the gait-design parameters. We will investigate the mutual effect of the robot speed and crawling success in the future, to obtain the maximum safe robot operating speed.

The presented results are fundamental to effectively deploy the robot in a real-world environment. However, multiple factors are critical and hence require consideration, before further developing iCrawl. Here, we describe the requirements for the successful *deployment* of iCrawl on metal pipes in a real-world scenario:

1. Its feet should adapt to varying curved surfaces. This is achieved by using the foot-caps.
2. It should have a sufficient and compact adhesion mechanism. This is achieved by using a single electromagnet for each foot.
3. Given the limitations of pneumatically actuated systems and other methods, an all-electrically driven robot offers greater deployment feasibility with the possibility of mounting all components onboard. This is achieved by a single DC battery powering all the system components.
4. It should distinguish between a metal and a non-metal pipe surface to keep the robot functional in a tested setting. This is achieved with the use of hall sensors.
5. It should be equipped with sufficient sensing methods to develop obstacle avoidance and other complex locomotion scenarios, ideally based on closed-loop control. This feature will be implemented in the future.
6. It should keep a stable and correct posture in cases of sudden external perturbation during crawling and the climbing. This is achieved by developing teleoperated posture control, however, it will be further developed to become autonomous.

According to the *deployability* requirements, we will work on points 5 and 6 in future. Furthermore, it is critical that the robot be self-learning for better path planning when negotiating obstacles in an unknown cluttered environment. In the

future, we intend to use a neural controller [38], [39], [41] to coordinate all the sensorimotor processes simultaneously. It will involve self-learning for autonomous crawling and the appropriate selection of gaits, depending on the surface, and the desired locomotion type (crawling, climbing, obstacle avoidance, etc.). To improve robot stability in the event of external perturbations during crawling/climbing, we will apply muscle models [40] to obtain compliant joint motions of the robot.

It should be noted that during the horizontal locomotion experiments, $M_{2,4}$ motor joints were locked into a certain position to facilitate unidirectional crawling. In the future, we will use these motor joints to obtain bi-directional body-rotation and hence versatile robot postures. This will improve the robot's ability to negotiate a multi-obstacle avoidance scenario during locomotion. We will also consider improving the design of the robot feet by developing a varying stiffness elastomeric toe that can act as a damper; reducing the foot-magnet impact on the surface while further improving the robot's stability and versatility for most surfaces. Further work on optimizing the various gait parameters through consideration of the power consumption in different scenarios will improve robot efficiency; contributing to the goal of an effective and autonomous pipeline inspection.

VI. CONCLUSION

We have presented a new design for an inchworm-inspired metal-pipe crawling robot. Development of the robot design and control was inspired by the biology of an inchworm. The robot crawled on metal pipes of different diameters as well as flat metal surfaces using two gaits and the proposed robot foot-caps. Robot gaits 1 and 2 show stepping and sliding-like movements, respectively. Robot gait 2 was proven to be effective on all the tested metal surfaces. Using the foot-caps, robot crawling improved in the tested scenarios. Gait 1 showed a lack of effectiveness in robot crawling when tested on the painted metal pipes. However, it was equally as effective as gait 2, when tested on non-painted metal surfaces. We proposed the use of foot-caps with gait 2 to achieve horizontal and vertical robot crawling/climbing on metal pipes. The presented results effectively improve the multi-curvature metal pipe crawling of the robot and can be built upon to efficiently deploy the robot in a real-world environment.

This work provides a baseline for further development of the robot for deployment in a multi-robot industrial pipe inspection. We anticipate that future development based on the presented results will effectively mitigate the tedious inspection workload of human site operators. We intend to deploy a drone to transport iCrawl to various targeted inspection locations. By using the drone, we anticipate a reduction in the travel time of iCrawl to assist the inspection of remotely located sites. The drone could also assist inspection on a broader level. However, closer pipe inspection could be effectively achieved by the iCrawl robot once it is further developed and meets all the *deployability* conditions described in this article. A concept animation of this multi-robot automated industrial pipe inspection can be seen at: http://www.manoonpong.com/icrawl/S5.mp4

ACKNOWLEDGMENT

The authors are grateful to Stephen John Turner, Supasorn Suwajanakorn, and Theerawit Wilaiprasitporn for their participation in the valuable discussions at various stages of the work. They also thank FIGO company for participating in technical discussions, and PTT Exploration and Production Public Company Ltd., for taking part in general discussions and providing the industrial pipes for robot testing.

REFERENCES

[1] F. Delcomyn, *Biologically Inspired Robots, Bioinspiration and Robotics Walking and Climbing Robots*, M. K. Habib, Ed. London, U.K.: IntechOpen, 2007. [Online]. Available: https://www.intechopen.com/books/bioinspiration_and_robotics_walking_and_climbing_robots/biologically_inspired_robots, doi: 10.5772/5506.

[2] R. Mukherjee, S. Vaughn, and B. A. Trimmer, "The neuromechanics of proleg grip release," *J. Experim. Biol.*, vol. 221, no. 13, Jul. 2018, Art. no. jeb173856, doi: 10.1242/jeb.173856.

[3] S. C. Vaughan, H.-T. Lin, and B. A. Trimmer, "Caterpillar climbing: Robust, tension-based omni-directional locomotion," *J. Insect Sci.*, vol. 18, no. 3, Jun. 2018, doi: 10.1093/jisesa/iey055.

[4] W. Wang, J.-Y. Lee, H. Rodrigue, S.-H. Song, W.-S. Chu, and S.-H. Ahn, "Locomotion of inchworm-inspired robot made of smart soft composite (SSC)," *Bioinspiration Biomimetics*, vol. 9, no. 4, Oct. 2014, Art. no. 046006, doi: 10.1088/1748-3182/9/4/046006.

[5] J. Zhang, T. Wang, J. Wang, B. Li, J. Hong, J. X. J. Zhang, and M. Y. Wang, "Dynamic modeling and simulation of inchworm movement towards bio-inspired soft robot design," *Bioinspiration Biomimetics*, vol. 14, no. 6, Sep. 2019, Art. no. 066012, doi: 10.1088/1748-3190/ab3e1f.

[6] P. Chattopadhyay, A. Majumder, H. Dikshit, S. K. Ghoshal, and A. Maity, "A bio-inspired climbing robot: Design, simulation, and experiments," *IOP Conf. Series, Mater. Sci. Eng.*, vol. 377, Jun. 2018, Art. no. 012105, doi: 10.1088/1757-899X/377/1/012105.

[7] E. Avila, A. Melendez, and M. Falfan, "An inchworm-like robot prototype for robust exploration," in *Proc. Electron., Robot. Automot. Mech. Conf. (CERMA)*, Sep. 2006, pp. 91–96, doi: 10.1109/CERMA.2006.13.

[8] Y.-Y. Yuan, W.-C. Lu, C.-J. Kao, J.-J. Hung, and P.-C. Lin, "Design and implementation of an inchworm robot," in *Proc. Int. Conf. Adv. Robot. Intell. Syst. (ARIS)*, Aug. 2016, p. 1, doi: 10.1109/ARIS.2016.7886615.

[9] K. Kotay and D. Rus, "The Inchworm Robot: A Multi-Functional System," *Auto. Robots*, vol. 8, no. 1, pp. 53–69, Jan. 2000, doi: 10.1023/A:1008940918825.

[10] B. Shin, J. Ha, M. Lee, K. Park, G. H. Park, T. H. Choi, K.-J. Cho, and H.-Y. Kim, "Hygrobot: A self-locomotive ratcheted actuator powered by environmental humidity," *Sci. Robot.*, vol. 3, no. 14, Jan. 2018, Art. no. eaar2629, doi: 10.1126/scirobotics.aar2629.

[11] J.-S. Koh and K.-J. Cho, "Omega-shaped inchworm-inspired crawling robot with Large-Index-and-Pitch (LIP) SMA spring actuators," *IEEE/ASME Trans. Mechatronics*, vol. 18, no. 2, pp. 419–429, Apr. 2013, doi: 10.1109/TMECH.2012.2211033.

[12] J. Ning, C. Ti, and Y. Liu, "Inchworm inspired pneumatic soft robot based on friction hysteresis," *J. Robot. Autom.*, vol. 1, no. 1, pp. 54–63, Sep. 2017.

[13] I. H. Han, H. Yi, C.-W. Song, H. E. Jeong, and S.-Y. Lee, "A miniaturized wall-climbing segment robot inspired by caterpillar locomotion," *Bioinspiration Biomimetics*, vol. 12, no. 4, Jun. 2017, Art. no. 046003, doi: 10.1088/1748-3190/aa728c.

[14] S. Rozen-Levy, W. Messner, and B. A. Trimmer, "The design and development of branch bot: A branch-crawling, caterpillar-inspired, soft robot," *Int. J. Robot. Res.*, May 2019, Art. no. 027836491984635, doi: 10.1177/0278364919846358.

[15] W. Wang, K. Wang, and H. Zhang, "Crawling gait realization of the mini-modular climbing caterpillar robot," *Prog. Natural Sci.*, vol. 19, no. 12, pp. 1821–1829, Dec. 2009, doi: 10.1016/j.pnsc.2009.07.009.

[16] M. H. Chang, S. H. Chae, H. J. Yoo, S.-H. Kim, W. Kim, and K.-J. Cho, "Loco-sheet: Morphing inchworm robot across rough-terrain," in *Proc. 2nd IEEE Int. Conf. Soft Robot. (RoboSoft)*, Apr. 2019, pp. 808–813, doi: 10.1109/ROBOSOFT.2019.8722724.

[17] Y. Yang, D. Li, and Y. Shen, "Inchworm-inspired soft robot with light-actuated locomotion," *IEEE Robot. Autom. Lett.*, vol. 4, no. 2, pp. 1647–1652, Apr. 2019, doi: 10.1109/LRA.2019.2896917.

[18] F. Moreira, A. Abundis, M. Aguirre, J. Castillo, and P. A. Bhounsule, "An inchworm-inspired robot based on modular body, electronics and passive friction pads performing the two-anchor crawl gait," *J. Bionic Eng.*, vol. 15, no. 5, pp. 820–826, Sep. 2018, doi: 10.1007/s42235-018-0069-x.

[19] H. Ogai and B. Bhattacharya, "Pipe inspection robots for gas and oil pipelines," in *Pipe Inspection Robots for Structural Health and Condition Monitoring*, H. Ogai and B. Bhattacharya, Eds. New Delhi, India: Springer, vol. 2018, pp. 13–43.

[20] A. Shukla and H. Karki, "Application of robotics in onshore oil and gas industry—A review part I," *Robot. Auto. Syst.*, vol. 75, pp. 490–507, Jan. 2016, doi: 10.1016/j.robot.2015.09.012.

[21] S. Jordan, J. Moore, S. Hovet, J. Box, J. Perry, K. Kirsche, D. Lewis, and Z. T. H. Tse, "State-of-the-art technologies for UAV inspections," *IET Radar, Sonar Navigat.*, vol. 12, no. 2, pp. 151–164, Feb. 2018, doi: 10.1049/iet-rsn.2017.0251.

[22] D. Schmidt and K. Berns, "Climbing robots for maintenance and inspections of vertical structures—A survey of design aspects and technologies," *Robot. Auto. Syst.*, vol. 61, no. 12, pp. 1288–1305, Dec. 2013, doi: 10.1016/j.robot.2013.09.002.

[23] S. M. Felton, M. T. Tolley, C. D. Onal, D. Rus, and R. J. Wood, "Robot self-assembly by folding: A printed inchworm robot," in *Proc. IEEE Int. Conf. Robot. Autom.*, May 2013, pp. 277–282, doi: 10.1109/ICRA.2013.6630588.

[24] P. H. Ward, P. Manamperi, P. Brooks, P. Mann, W. Kaluarachchi, L. Matkovic, G. Paul, C. Yang, P. Quin, D. Pagano, and D. Liu, "Climbing robot for steel bridge inspection: Design challenges," in *Proc. Austroads Bridge Conf.*, 2014, pp. 1–13.

[25] H. Zhu, Y. Guan, W. Wu, L. Zhang, X. Zhou, and H. Zhang, "Autonomous pose detection and alignment of suction modules of a biped wall-climbing robot," *IEEE/ASME Trans. Mechatronics*, vol. 20, no. 2, pp. 653–662, Apr. 2015, doi: 10.1109/TMECH.2014.2317190.

[26] H. Ko, H. Yi, and H. E. Jeong, "Wall and ceiling climbing quadruped robot with superior water repellency manufactured using 3D printing (UNIclimb)," *Int. J. Precis. Eng. Manuf.-Green Technol.*, vol. 4, no. 3, pp. 273–280, Jul. 2017, doi: 10.1007/s40684-017-0033-y.

[27] W. Fischer, F. Tâche, and R. Siegwart, "Magnetic Wall Climbing Robot for Thin Surfaces with Specific Obstacles," in *Proc. 6th Int. Conf. Field Service Robot., Results*, C. Laugier and R. Siegwart, Eds. Berlin, Germany: Springer, 2008, pp. 551–561.

[28] T. Bandyopadhyay, R. Steindl, F. Talbot, N. Kottege, R. Dungavell, B. Wood, J. Barker, K. Hoehn, and A. Elfes, "Magneto: A versatile multi-limbed inspection robot," in *Proc. IEEE/RSJ Int. Conf. Intell. Robots Syst. (IROS)*, Oct. 2018, pp. 2253–2260, doi: 10.1109/IROS.2018.8593891.

[29] Y. Liu, H. Kim, and T. Seo, "AnyClimb: A new wall-climbing robotic platform for various curvatures," *IEEE/ASME Trans. Mechatronics*, vol. 21, no. 4, pp. 1812–1821, Aug. 2016, doi: 10.1109/TMECH.2016.2529664.

[30] K. Nagaoka, H. Minote, K. Maruya, Y. Shirai, K. Yoshida, T. Hakamada, H. Sawada, and T. Kubota, "Passive spine gripper for free-climbing robot in extreme terrain," *IEEE Robot. Autom. Lett.*, vol. 3, no. 3, pp. 1765–1770, Jul. 2018, doi: 10.1109/LRA.2018.2794517.

[31] M. Tavakoli, C. Viegas, L. Marques, J. N. Pires, and A. T. de Almeida, "OmniClimbers: Omni-directional magnetic wheeled climbing robots for inspection of ferromagnetic structures," *Robot. Auto. Syst.*, vol. 61, no. 9, pp. 997–1007, Sep. 2013, doi: 10.1016/j.robot.2013.05.005.

[32] M. Osswald and F. Iida, "Design and control of a climbing robot based on hot melt adhesion," *Robot. Auto. Syst.*, vol. 61, no. 6, pp. 616–625, Jun. 2013, doi: 10.1016/j.robot.2013.02.004.

[33] K. Nagaya, T. Yoshino, M. Katayama, I. Murakami, and Y. Ando, "Wireless piping inspection vehicle using magnetic adsorption force," *IEEE/ASME Trans. Mechatronics*, vol. 17, no. 3, pp. 472–479, Jun. 2012, doi: 10.1109/TMECH.2011.2182201.

[34] J. Lim, H. Park, J. An, Y.-S. Hong, B. Kim, and B.-J. Yi, "One pneumatic line based inchworm-like micro robot for half-inch pipe inspection," *Mechatronics*, vol. 18, no. 7, pp. 315–322, Sep. 2008, doi: 10.1016/j.mechatronics.2008.05.007.

[35] W. Neubauer, "Locomotion with articulated legs in pipes or ducts," *Robot. Auton. Syst.*, vol. 11, no. 3, pp. 163–169, Dec. 1993, doi: 10.1016/0921-8890(93)90021-4.

[36] B. L. Luk, D. S. Cooke, S. Galt, A. A. Collie, and S. Chen, "Intelligent legged climbing service robot for remote maintenance applications in hazardous environments," *Robot. Auto. Syst.*, vol. 53, no. 2, pp. 142–152, Nov. 2005, doi: 10.1016/j.robot.2005.06.004.

[37] M. B. Khan, J. C. Larsen, and P. Manoonpong, "An ant-inspired control strategy for active sensing of a crawling robot in a cluttered environment," in *Proc. 9th Int. Symp. Adapt. Motion Animals Mach. (AMAM)*, 2019. Accessed: Nov. 7, 2019. [Online]. Available: https://infoscience.epfl.ch/record/271269

[38] P. Manoonpong, *Neural Preprocessing and Control of Reactive Walking Machines: Towards Versatile Artificial Perception-Action Systems* (Cognitive Technologies). Berlin, Germany: Springer-Verlag, 2007.

[39] P. Manoonpong, F. Pasemann, and F. Wörgötter, "Sensor-driven neural control for omnidirectional locomotion and versatile reactive behaviors of walking machines," *Robot. Auto. Syst.*, vol. 56, no. 3, pp. 265–288, Mar. 2008, doi: 10.1016/j.robot.2007.07.004.

[40] X. Xiong, F. Worgotter, and P. Manoonpong, "Adaptive and energy efficient walking in a hexapod robot under neuromechanical control and sensorimotor learning," *IEEE Trans. Cybern.*, vol. 46, no. 11, pp. 2521–2534, Nov. 2016, doi: 10.1109/TCYB.2015.2479237.

[41] P. Ngamkajornwiwat, J. Homchanthanakul, P. Teerakittikul, and P. Manoonpong, "Bio-inspired adaptive locomotion control system for online adaptation of a walking robot on complex terrains," *IEEE Access*, vol. 8, pp. 91587–91602, 2020, doi: 10.1109/ACCESS.2020.2992794.

MUHAMMAD BILAL KHAN received the B.Eng. degree (Hons.) in electrical and electronic engineering from the University of Bradford, U.K., in 2016, and the M.Eng. (Research) degree in mechanical engineering from the Prince of Songkla University, Thailand, in 2018. He is currently with the Bioinspired Robotics and Neural Engineering (BRAIN) Laboratory, School of Information Science and Technology, VISTEC, Thailand. His current research interest includes design and control of robots via bio-inspired approaches.

THIRAWAT CHUTHONG received the bachelor's degree (Hons.) in robotics and automation engineering from the King Mongkut's University of Technology at Thonburi, Thailand, in 2019. He has worked as a System Engineering Intern with Venus Supply Company Ltd., Thailand, in 2018. He is currently a Research Engineer with the Bioinspired Robotics and Neural Engineering (BRAIN) Laboratory, School of Information Science and Technology, VISTEC, Thailand. His previous work includes design and system integration of multi DOF robots. His research interest includes the research on the design of the legged robots.

CAO DANH DO received the B.Eng. degree in mechanical engineering and the M.Sc. degree in structural engineering from the University of Southern Denmark (SDU), Odense, Denmark, in 2012 and 2014, respectively. He is currently a Research Assistant with the SDU Biorobotics Group. For four years, he has worked as a Consultant with machinery systems and arrangements within the maritime industry. During the last two years, his focus has shifted towards contributing to designing and building bio-inspired robots and other mechanisms through the group's many prototyping activities. His current research interests include mechanism design, fabrication methods, rapid prototyping, and topology optimization.

MATHIAS THOR received the M.Sc. degree in robot systems from the University of Southern Denmark, Odense, Denmark, in 2019, where he is currently pursuing the Ph.D. degree with SDU Embodied Systems for Robotics and Learning. His current research interests include neural locomotion control of walking machines, learning/plasticity, dynamic simulations, and design of legged robotic systems, including their software interface. During his Ph.D. degree, he has won several awards, including the EliteForsk Travel Grant from the Ministry of Higher Education and Science of Denmark.

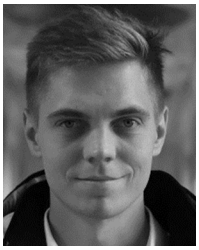

PETER BILLESCHOU received the M.Sc. degree in biomedical engineering from the University of Strathclyde, U.K., in 2014. He is currently pursuing the Ph.D. degree in the D-Life project with SDU BioRobotics, University of Southern Denmark. He has since worked on the development of medical thoracic implants, hydraulic actuators, components for industrial robots, ensuring CE marking, as well as being a Consultant in the health tech industry. His current research interests include morphology optimization of walking machines, biomechanics, proprioceptive actuators, underactuated systems, compliant mechanisms, superelastic materials, as well as environmental resilient sensors and mechanisms for robots.

JØRGEN CHRISTIAN LARSEN received the B.Eng. degree in science in computer systems engineering, the M.Sc. degree in robot systems engineering, and the Ph.D. degree in robotic systems on the EU Project Locomorph from The Maersk Mc-Kinney Moller Institute, University of Southern Denmark, in 2008, 2011, and 2013, respectively. He is currently an Associate Professor in embedded electronics and artificial intelligence with the University of Southern Denmark. He is also an Adjunct Professor with the School of Information Science and Technology, Vidyasirimedhi Institute of Science and Technology (VISTEC), Thailand. His research interests include embodied artificial intelligence, embedded electronics, FPGA control and design, cyber-physical systems, mechanical design of walking machines, soft robotics, and educational research.

PORAMATE MANOONPONG (Member, IEEE) received the Ph.D. degree in electrical engineering and computer science from the University of Siegen, Siegen, Germany, in 2006. He was the Emmy Noether Research Group Leader for neural control, memory, and learning for complex behaviors in multisensory-motor robotic systems with the Bernstein Center for Computational Neuroscience, Georg-August Universitaet Goettingen, Goettingen, Germany, from 2011 to 2014. He is currently a Professor with the School of Information Science and Technology, Vidyasirimedhi Institute of Science and Technology (VISTEC), Thailand. He has also served as an Associate Professor of embodied AI and robotics with the University of Southern Denmark (SDU), Denmark, and a Professor with the College of Mechanical and Electrical Engineering, Nanjing University of Aeronautics and Astronautics (NUAA), China. His current research interests include embodied AI, machine learning for robotics, neural locomotion control of walking machines, biomechanics, dynamics of recurrent neural networks, learning/plasticity, embodied cognitive systems, prosthetic and orthopedic devices, exoskeletons, brain–machine interface, human–machine interaction, and service/inspection robots.